Atoms riding Rayleigh waves

2010 J. Phys.: Condens. Matter 22 304016

(http://iopscience.iop.org/0953-8984/22/30/304016)

IOP PUBLISHING JOURNAL OF PHYSICS: CONDENSED MATTER

J. Phys.: Condens. Matter **22** (2010) 304016 (11pp) doi:10.1088/0953-8984/22/30/304016

Atoms riding Rayleigh waves

G Benedek[1,5], P M Echenique[1,2], J P Toennies[3] and F Traeger[4]

[1] Donostia International Physics Center (DIPC), 20018 Donostia-San Sebastián, Spain
[2] Departamento de Física de Materiales and CFM (CSIC-UPV/EHU), Universidad del País Vasco/Euskal Herriko Unibertsitatea, E-20018 San Sebastián/Donostia, Spain
[3] Max Planck-Institut für Dynamik und Selbstorganisation, D-37073 Göttingen, Germany
[4] Fakultät für Chemie und Biochemie, Ruhr-Universität Bochum, Universitätsstraße 150, D-44801 Bochum, Germany

Received 1 March 2010, in final form 15 April 2010
Published 13 July 2010
Online at stacks.iop.org/JPhysCM/22/304016

Abstract

Under special kinematic conditions helium atoms impinging upon a crystal surface can be inelastically trapped into a surface bound state and ride the created Rayleigh wave. This special case of phonon-assisted selective adsorption, leading to an atom–phonon bound state (*atomic polaron*), can explain previously unassigned resonant features observed in published helium atom scattering distributions.

(Some figures in this article are in colour only in the electronic version)

1. Introduction

Surface acoustic waves (SAW) in semiconductors can trap electrons and holes in their deformation potential and carry them along the surface. This phenomenon, known as the *acoustoelectric effect* or *acoustoconductance*, was recognized about two decades ago [1–7] and exploited in various applications, ranging from optoelectronic systems [8, 9] to single-electron transport [10, 11] and quantum computation [12–15]. Although in these works SAWs are generated by external sources, surface electrons can also be trapped by a surface phonon that the electron itself has excited with its Coulomb field (*self-trapping*) [16]. The extension of SAWs into the THz domain, where dispersive and quantum effects are important, is now benefiting from the knowledge acquired about surface phonons in 30 years of helium atom scattering (HAS) [17] and high-resolution electron energy loss (HREELS) spectroscopy [18, 19]. Inspired by the electron experiment of Ge *et al* [16], a natural question to ask is whether an He atom trapped in a bound state by phonon-assisted selective adsorption can be carried along by the phonon wave that the atom itself has created. Before answering this question a brief introduction to HAS physics and inelastic selective adsorption is in order.

The pioneering theory by Manson and Celli on the inelastic scattering of atoms from crystal surfaces [20–22] constituted the basis for the development of surface phonon spectroscopy by helium atom scattering (HAS) [23–26] and provided a firm starting point for further theoretical studies of HAS from real crystal surfaces and realistic gas surface potentials [26, 17]. The complex dynamics of inelastic atom scattering from periodic crystal surfaces arising from the interplay of surface corrugation, surface phonons and atom bound states gives rise to a variety of resonance and focusing phenomena. The diagrams of figure 1 illustrate the *energy loss* as a function of the *parallel momentum (wavevector) transfer* in various focusing phenomena occurring in inelastic atom scattering from a crystal surface. In all the processes shown in figure 1 the incident energy E_i and parallel momentum $\hbar K_i$ of the atom are converted into the final energy E_f and parallel momentum $\hbar K_f$ by creating a phonon of energy $\hbar\omega(Q)$ traveling in the forward direction with a wavevector Q. For the present discussion it is convenient to represent the forward creation processes in the first quadrant of the phonon momentum–energy plane ($Q, \hbar\omega(Q) > 0$), as in the original definition of scan curves [27], rather than in the third quadrant ($Q < 0, \hbar\omega(Q) < 0$) as usually done in the analysis of HAS spectra [23–25].

Annihilation and backward propagation can be accounted for by extending figures 1(a)–(d) to negative energy and momentum axes. The *scan curve s* links all the possible energy losses to the corresponding parallel momentum losses in inelastic HAS for a given scattering geometry and incident angles [27]. Its intersections with the dispersion curves of surface phonons (S) and the bulk phonon continuum (B) correspond to single peaks and an extended band in the observed time-of-flight (TOF) spectrum, respectively. The curves r_n ($n = 1, 2$) have a similar meaning as the scan curve,

[5] Permanent address: Dipartimento di Scienza dei Materiali, Universitá di Milano-Bicocca, Via Cozzi 53, 20125 Milano, Italy.

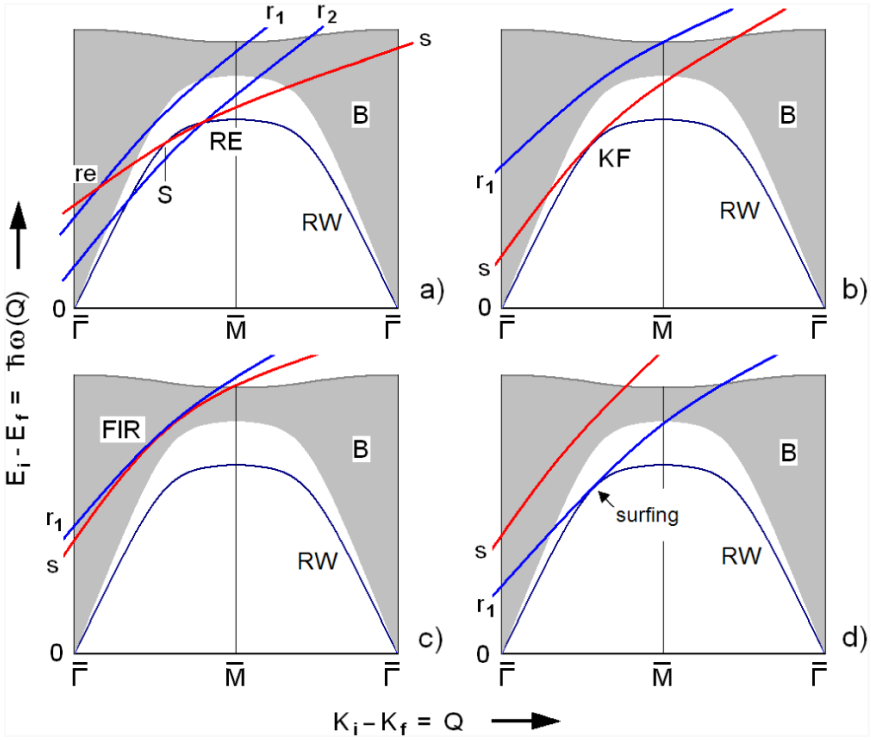

Figure 1. Diagrams illustrating the energy loss as a function of the parallel momentum (wavevector) loss in various HAS focusing phenomena involving the creation of a phonon of energy $\hbar\omega(Q)$ and wavevector Q. The *scan curve s*, which depends on the scattering geometry and incident energy, links the possible energy losses to the parallel momentum losses corresponding to scattering in which the particle arrives at the detector. The intersections (S) of the scan curve with a surface phonon dispersion curve (RW) and the bulk phonon continuum (B) determine the features of inelastic time-of-flight spectra. The curves r_1 and r_2 link the energy loss to the parallel momentum transfer for inelastic (phonon-assisted) selective adsorption into different bound states. (a) The intersection of s with the surface phonon branch represents an ordinary inelastic process, whereas the double intersection of s and r_2 with RW determines a resonance-enhanced (RE) inelastic process. (b) The tangency of a scan curve with a phonon branch causes a kinematical focusing (KF) yielding a peculiar saw-tooth peak in the angular distribution (AD). (c) The tangency of s with r_1 inside the bulk phonon continuum gives a focused inelastic resonance (FIR), with a peculiar feature in the AD at a fixed angle. (d) The tangency of r_1 with a surface phonon branch leads to the surfing phenomenon discussed in this paper.

where, however, the final state of the He atom is a bound state of energy $-|\varepsilon_n| + \hbar^2 K_f^2/2m^*$, with $\hbar K_f$ the final parallel wavevector and m^* the effective mass of the He atom in the bound state. Once trapped in the bound state the particle is eventually scattered incoherently and thus does not arrive at the detector. This state can be accessed by the incident atom via an inelastic (phonon-assisted) selective adsorption, with or without a surface reciprocal lattice vector. In figure 1(a) the intersection of s with the surface phonon branch (S) represents an ordinary inelastic process, whereas the double intersection of s and r_2 with S determines a resonance enhancement (RE) of the phonon peak in the time-of-flight spectrum. The $s - r_1$ intersection (re) within the bulk continuum also yields a resonance enhancement at some energy in the continuous bulk phonon spectrum. The enhancement is said to be resonant because the atom, which entered inelastically a bound state and is then elastically desorbed towards the detector, has followed a path alternative to the direct inelastic scattering; this additional channel interferes with the direct one and gives a Fano resonance (*inelastic bound state resonance*) in the angular distribution (AD) [28, 29] as well as in the TOF spectrum [29–31]. The tangency of a scan curve with a phonon branch (figure 1(b)) yields a peculiar saw-tooth peak in the scattering angular distribution (AD), a phenomenon known as *kinematical focusing* (KF) [27, 32]. Also the tangency of s with r_1 inside the bulk phonon continuum (figure 1(c)) determines a peculiar feature in the AD at a fixed angle called *focused inelastic resonance* (FIR) [33–37]. Finally the tangency of r_1 with a surface phonon branch (figure 1(d)) yields the *surfing effect* investigated in the present paper. The special case where the scan curve crosses the surfing tangency point corresponds to the resonant focusing (RF). The RF was first predicted by Miret-Artés [38] as a special case of an inelastic resonance, where the atom is re-emitted towards the detector. The latter condition in planar scattering and fixed incident energy is generally not fulfilled since only the incident angle can be varied, and the surfing effect is signaled by a minimum in the angular distribution. However, in the special case of RF the re-emission of the surfing atom towards the detector yields a maximum.

Phonon-assisted bound state resonances have important effects on the sticking coefficient and on the fraction of atoms which are elastically scattered, expressed by the Debye–Waller (DW) factor. Šiber and Gumhalter, through both quantum-mechanical and semiclassical calculations of the DW factor, showed that the sticking of rare-gas atoms on flat metal

surfaces, where the static corrugation is negligible and no elastic selective adsorption (SA) is possible, mostly occurs via the assistance of RWs [39]. In a further study Šiber *et al* have discussed the kinematic effects on the DW factor and sticking in connection with HAS from an Xe overlayer on Cu(111) [40]. The calculation of the DW exponent as a function of the incident energy shows peaks associated with SA into bound states assisted by single phonons of the Xe overlayer dispersionless (Einstein) branch with shear-vertical polarization [40]. Technically each peak corresponds to the tangency of the flat phonon branch with the maximum of the inelastic resonance curve r_n for the nth bound state ($n = 1, 2$ in Šiber *et al* [40]), thus fulfilling the surfing condition. For a flat branch, however, the tangency condition is independent of the incident angle and can be met only by changing the incident energy, though the largest effect on the DW exponent occurs at normal incidence [40]. In the case of normal incidence and one single oscillator mimicking an Einstein phonon branch the scattering problem is reduced to a set of one-dimensional (1D) coupled channel equations, allowing for a virtually exact calculation of the *multiphonon* resonances in the DW factor [41, 42]. A surprising result is the suppression or reduction of the inelastic scattering at resonant incident energies. In the 1D case the Fano resonances turn out to be very sharp and intense, but are much reduced in 2D and almost completely suppressed in 3D, as shown by Šiber and Gumhalter with a restricted Fock space-coupled channel (RFCC) calculation [43, 44]. These recent advances in the theory of phonon-assisted bound state resonances in atom surface scattering are summarized and carefully discussed in [45].

The inelastic bound state resonances and the focusing effects, nicely encompassed by Miret-Artés within a comprehensive mathematical theory of the *critical kinematical effects* [38, 46–49], have been accurately described in connection with the development of HAS surface phonon spectroscopy. Along this line of thought Miret-Artès and Manson have developed the theory of focusing effects occurring at special values of the incident angle or energy in the sticking via elastic SA, under conditions similar to the rainbow effect [50], or via the exchange of a fixed amount of energy with the phonon system [51].

The inelastic bound state resonances have been exploited to enhance the inelastic HAS signal, which led to the detection of optical surface phonons [52, 53]. The intriguing question whether a final scattering state of the atom in resonance with a surface bound state yields a visible signal in the angular distribution was raised by Lilienkamp and Toennies [29] in connection with the *selective desorption* [54]. One may argue that, in inelastic HAS processes, where atoms of energy E_i arrive at a fixed incident angle θ_i and leave at a fixed final angle θ_f, the final energies E_f have, in general, a continuum of possible values, and only one at most of these final states can match the resonance condition with a given surface bound state. Thus no distinct feature would be expected in angular distributions from selective desorption processes. Lilienkamp and Toennies showed, however, that selective desorption can yield sharp features in the angular distribution when both the incident and the scattered beams are in resonance with a bound state, a special *double-resonance* condition pictorially termed a *supernova* [29]. The spectacular supernova intensity observed in the angular distribution of LiF(001) was subsequently recognized to be associated with FIR [33]. Altogether the various bound state resonances and focusing processes mentioned above provide a rather precise and complete account of the sharp features observed in the HAS angular distributions. However, the HAS angular distributions of the ionic surfaces thoroughly investigated, notably NaF(001) [24, 32], LiF(001) [23, 31], NaCl(001) [34, 55] and MgO(001) [56][5], show a few sharp dips which remained unassigned.

The new analysis in this work provides the first evidence of the surfing process in which an impinging atom is selectively adsorbed into a bound state with the aid of a surface phonon. The phonon can provide the necessary parallel momentum and energy to fulfill energy and parallel momentum conservation; thus the process can occur even without the exchange of a surface reciprocal lattice vector (**G**-vector), which is instead required for an ordinary (elastic) SA process. When no **G**-vector is involved or a **G**-vector normal to scattering plane is exchanged the planar component of the atom group velocity is found to be equal to the group velocity of the phonon involved in the inelastic selective adsorption. In this case the atom and the phonon wave travel together, just like in surfing, and form a type of bound state, much in the same way as the self-trapped electron in the experiments of Ge *et al* [16] forms *a small polaron* with the companion SAW [57].

2. Surfing conditions

Consider an atom of mass m, impinging upon a surface (figure 2) with an incident energy $E_\mathrm{i} = \hbar^2 k^2/2m$, an incident angle θ_i and the parallel component of the initial wavevector given by $K_\mathrm{i} = k_\mathrm{i} \sin\theta_\mathrm{i}$. This is selectively adsorbed into a surface bound state of total energy $-|\varepsilon_n| + \hbar^2 K_\mathrm{f}^2/2m^*$, where $-|\varepsilon_n|$ is the nth bound state level, $\hbar K_\mathrm{f}$ is the final momentum of the atom moving parallel to the surface and m^* is its effective mass for the motion in the bound state. The process is assumed to be inelastic and to involve the creation (or annihilation) of a surface phonon of frequency $\omega(Q)$ and parallel wavevector **Q**. It may occur without or with an exchange of a surface **G**-vector (normal or *umklapp* process, respectively). In the latter case the vector **G** is split into the planar ($G_\parallel$) and non-planar ($G_\perp$) components with respect to the incident plane. Conservation of energy and parallel momentum leads to the equation for the inelastic selective adsorption:

$$\hbar\omega(Q) = E_\mathrm{i} + |\varepsilon_n| - \frac{\hbar^2}{2m^*}[(k_\mathrm{i}\sin\theta_\mathrm{i} - G_\parallel - Q)^2 + G_\perp^2]. \quad (1)$$

This equation links the inelastic energy transfer $\hbar\omega(Q)$ to the phonon momentum $\hbar Q$, thus providing the *resonance curve* in the $(Q, \hbar\omega(Q))$ plane for inelastic SA processes (r_n in

[5] In this work the G-vectors labeling the SA resonances are different from those labeling the SA resonances in the present work, since the former were referring to the bulk crystallographic axes, whereas here both diffraction and SA resonances are consistently labeled by surface G-vectors.

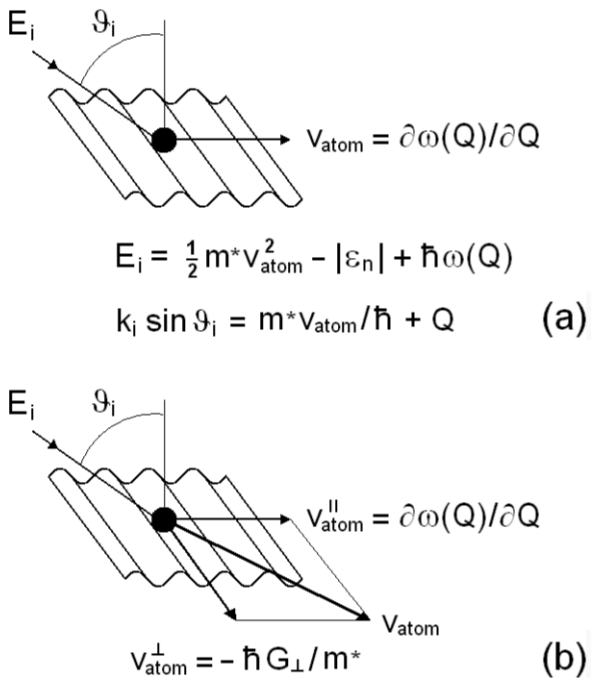

Figure 2. The surfing effect: (a) an atom impinging onto a surface is selectively adsorbed into a bound state $-|\varepsilon_n|$ via the excitation of a surface phonon of energy $\hbar\omega(Q)$ and wavevector Q, which is here represented by a traveling wave. For special values of the incident angle ϑ_i or energy E_i the atom and the surface phonon wave have the same group velocity and travel together, with the atom trapped in a trough of the surface phonon wave. (b) The inelastic selective adsorption may also occur with the concurrent exchange of a surface reciprocal lattice vector **G**. Under surfing conditions with a **G**-vector normal to the phonon wavevector a lateral (*tube-riding*) surfing occurs with the atom running in a trough of the surface phonon wave. The symbols are explained in the text.

figure 1). The possible processes are given by the intersections of the resonance curve with the phonon dispersion curves. It is convenient to represent the phonon dispersion curves in the four quadrants of the $(Q, \hbar\omega(Q))$ plane, i.e. for both positive and negative values of Q and $\hbar\omega(Q)$, so that all possible inelastic processes involving creation or annihilation of phonons in either forward or backward directions are considered. However, the effects discussed herein are seen to involve only phonon creation processes.

Surfing occurs when a resonance curve for the given incident energy and angle is tangent to a phonon dispersion curve. This means equality between the phonon group velocity and the slope of the resonance curve:

$$\mathbf{v}_{\rm phon}(Q) \equiv \frac{\partial\omega(Q)}{\partial Q} = \frac{\hbar}{m^*}(K_{\rm i} - Q - G_{\parallel}). \qquad (2)$$

The simultaneous fulfillment of equations (1) and (2) gives, for a given incident energy and each bound state level $-|\varepsilon_n|$, the incident angle at which the corresponding feature is found in the angular distribution. From the parallel momentum conservation for the planar and non-planar components, $K_{\rm f,\parallel} = K_{\rm i} - Q - G_{\parallel}$ and $K_{\rm f,\perp} = -G_{\perp}$, the atom group velocity in the planar direction:

$$\mathbf{v}_{\rm atom} \equiv \frac{\partial E_{\rm f}(\mathbf{K}_{\rm f})}{\hbar\partial K_{\rm f,\parallel}} = \frac{\hbar}{m^*}(K_{\rm i} - Q - G_{\parallel}), \qquad (3)$$

is seen to be equal to the phonon group velocity. This equality implies that the atom and the surface phonon travel together or, in other words, the atom is carried along the surface by the phonon, trapped in a potential minimum of the phonon wave. The image of an atom riding a phonon wave is quite natural. It should be noted that, unlike the elastic SA condition, equation (1) can be fulfilled also for $\mathbf{G} = 0$ (direct inelastic SA), provided the phonon energy is sufficiently large (figure 1(a)). Besides the direct process, *umklapp* processes involving a finite **G** are also possible. Among the *umklapp* processes, the one for $\mathbf{G} = (0, G_{\perp})$ corresponds to the atom carried by the surface phonon in a trough of the dynamic corrugation and rapidly moving along the trough in a direction normal to the phonon wavevector (figure 1(b)). Thus the surfing atom may also exhibit some carving and tube-riding abilities as an experienced surfer riding ocean waves.

In dealing with SA processes a relevant question is whether the features produced in the angular distribution for a given scattering geometry, e.g. the 90°-scattering geometry as in the experiments discussed below, are peaks or dips. When the bound state is involved in a resonant process, i.e. in a virtual transition from the incident beam to the bound state and back into the final beam, the interference between the direct scattering channel and the one through the bound state will give either a maximum or a minimum in the angular distribution, depending on the phase shift. In the present case, however, the atom is likely to be carried away beyond the beam coherence length and is lost for the scattered beam. Thus the surfing process should show up as a dip in the angular distribution, unlike the ordinary KF which yields an asymmetric peak [27, 32].

3. Experimental evidence of surfing

3.1. NaF(001)

In view of the large number of HAS investigations carried out in the past on corrugated surfaces such as those of alkali halides and some metal oxides, it is natural to verify whether some of the unassigned features in the angular distributions from those surfaces can be ascribed to the surfing process. The most interesting case is that of NaF(001), where the ordinary kinematical focusing (KF) with the Rayleigh wave (RW) dispersion curves was first demonstrated and thoroughly studied [32]. The features associated with the KF were identified in the angular distributions for planar scattering by rotating the azimuth of the incidence plane by a small amount (5°) away from a symmetry direction (figure 3). In this way the SA resonant features (peaks and dips) were largely suppressed due to the misalignment with the **G**-vectors required for the elastic SA processes, whereas the KF peaks remained practically unchanged and could be determined. The analysis of time-of-flight spectra for incident angles just below and above the KF angles confirmed the assignments. There

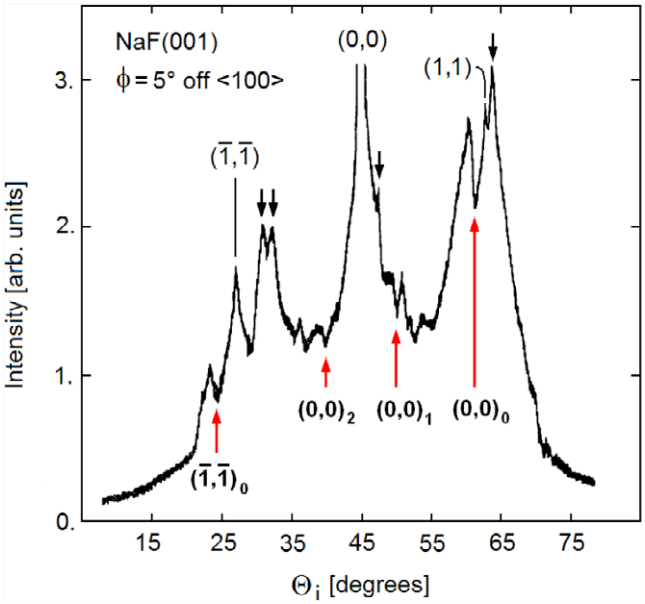

Figure 3. HAS angular distribution for NaF(001) at room temperature ($k_i = 6.01$ Å^{-1}) for planar scattering with the plane azimuth rotated by 5° with respect to the ⟨100⟩ direction in order to greatly reduce the diffraction and selective adsorption peaks [32]. In this way the kinematical focusing peaks (↓) and the dips corresponding to surfing states $(l, m)_n$ associated with the reciprocal lattice vector $G = (l, m)$ and the nth bound state level (↑) are clearly distinguished.

are, however, features in the rotated AD (figure 3), notably the dips marked by upward arrows, which cannot be attributed to KF (downward arrows) nor to the residual intensity of the diffraction peaks and of the (now out-of-plane) bound state resonances.

According to the analysis based on equations (1) and (2), the dips can instead be associated with phonon-assisted SA into surfing states. Figure 4 shows the resonance curves, equation (1), for the three bound states $-|\varepsilon_n|$ ($n = 0, 1, 2$) of NaF(001) ($\varepsilon_0 = -4.92$ meV, $\varepsilon_1 = -1.87$ meV, $\varepsilon_2 = -0.54$ meV [24]), and for $\mathbf{G} = 0$, the incident wavevector $k_i = 6.01$ Å^{-1}, and the scattering plane in the ⟨100⟩ direction (⟨11⟩ in two-dimensional coordinates). The incident angles 60.9°, 47.5°, 40.5° and 24.0°, chosen for the four panels of figure 4 in correspondence with the marked dips of figure 3, give a tangency of one of the three resonance curves with the dispersion curve of the Rayleigh waves (RW) [24]. The RW dispersion curve is plotted over more surface Brillouin zones (BZ) for phonon forward ($\partial\omega(Q)/\partial Q > 0$) and backward ($\partial\omega(Q)/\partial Q < 0$) creation or annihilation. It appears, however, that for 60.9°, 47.5° and 40.5° the tangency points are all in the first BZ ($\mathbf{G} = 0$) of the forward creation quadrant, respectively, for the deepest ($n = 0$) and the next ($n = 1, 2$) bound states. The tangency points are not intersected by the corresponding scan curves (s) and therefore represent three pure forward surfing states at fairly low group velocities (∼600 m s^{-1}). The dip in the AD at 24.0° corresponds instead to an *umklapp* process since a vector $\mathbf{G} = (\bar{1}, \bar{1})$ (in reciprocal vector units) has to be added in order to bring the tangency point into the first BZ. Note that the 24.0° surfing dip is visible even for the rotated azimuth where the $(\bar{1}, \bar{1})$ diffraction peak is almost completely suppressed (figure 3); this is due to the fact that the surfing atoms do not have to be reflected to the detector.

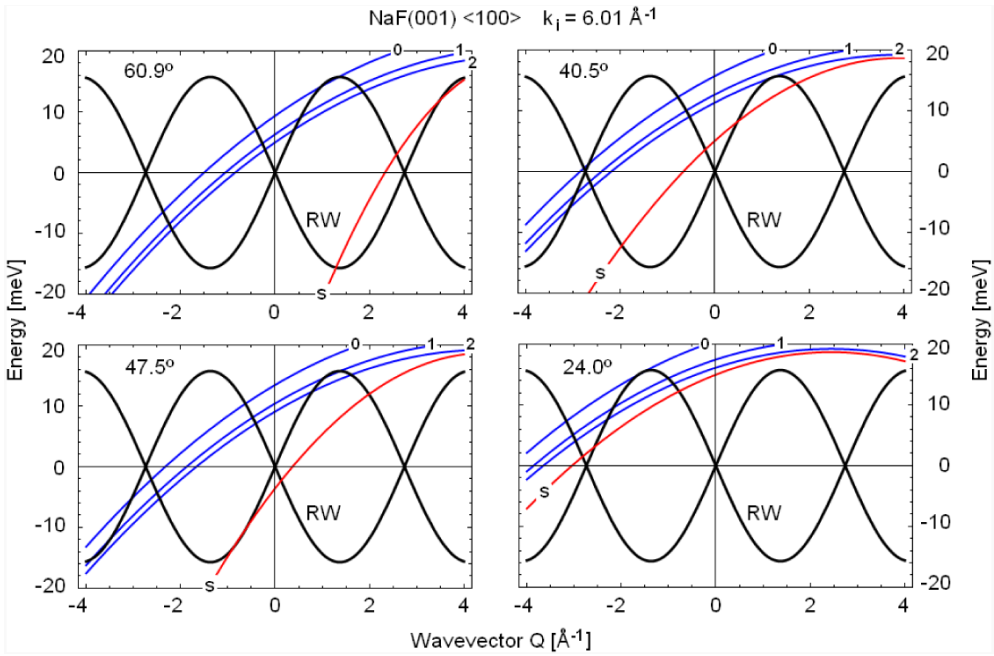

Figure 4. HAS scan curves (s) and resonance curves for the bound states $n = 0, 1, 2$ of He on NaF(001) along the ⟨100⟩ direction for an incident wavevector $k_i = 6.01$ Å^{-1} and incident angles of 60.9°, 47.5°, 40.5° and 24.0°. At each of these angles one of the resonant curves is tangent to the Rayleigh wave (RW) dispersion curve, thus fulfilling the condition for a surfing state. The corresponding dips in the AD are marked by an upward arrow in figure 3.

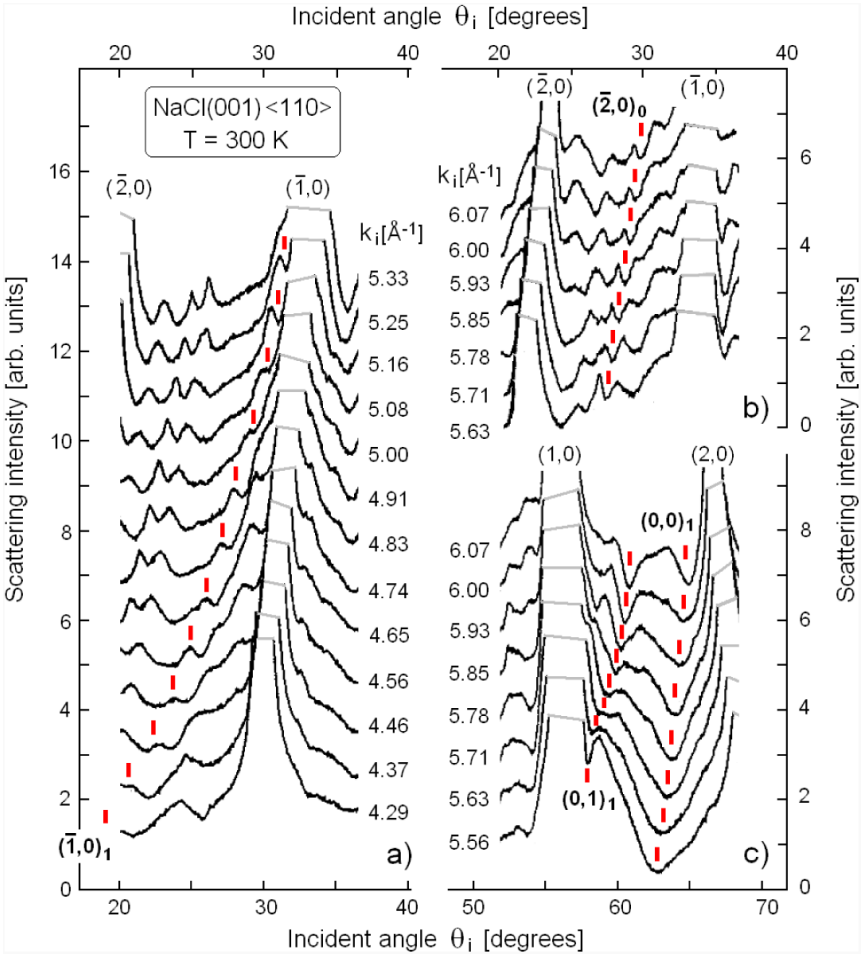

Figure 5. (a) Angular distributions of HAS from NaCl(001) in the ⟨110⟩ direction measured at room temperature for different incident wavevectors k_i and incident angles between the diffraction peaks $(\bar{2}, 0)$ and $(\bar{1}, 0)$ (adapted from [34]). (b) Same as (a) for higher values of k_i. (c) Same as (a) for larger incident angles between the diffraction peaks (1, 0) and (2, 0). Thick bars mark sequences of features assigned to $(\bar{1}, 0)_1$ (a), $(\bar{2}, 0)_0$ (b), $(0, 1)_1$ and $(0, 0)_1$ (c) surfing states. Surfing states are characterized by dips, but the sequence in (a) meets the RF condition for k_i between 4.5 and 5 Å^{-1} and the dips evolve into maxima.

3.2. NaCl(001)

Another way to distinguish surfing dips from the other features of the AD is to measure the shift of their angular positions as a function of the incident momentum k_i. Surfing dips and SA resonances shift in different ways and can be easily recognized. These kinds of measurements were previously made for NaCl(001) in the ⟨110⟩ direction in order to detect the FIR phenomenon [34]. Portions of the ADs reported in [34] for a thick mesh of k_i values are reproduced in figure 5. The deepest bound state levels of NaCl(001) are located at $\varepsilon_0 = -7.2$ meV, $\varepsilon_1 = -1.87$ meV and $\varepsilon_2 = -1.6$ meV [58]. Many of the features appearing in the ADs could not be assigned, including those marked by thick vertical bars in figure 5 and a few more which are not discussed here. The same analysis as carried out for NaF(001) ⟨100⟩ in the previous subsection now allows us to attribute most of the unassigned dips to direct and *umklapp* surfing processes. The most important ones are those belonging to the marked sequences measured at low incident angles (figures 5(a) and (b)) and large incident angles (figure 5(c)). At large incident angles (figure 5(c)) the two marked sequences $(0, 0)_1$ and $(0, \bar{1})_1$ correspond to a forward surfing state and to an oblique (*tube-riding*) surfing state with a perpendicular $\mathbf{G} = (0, 1)$, respectively, both involving the $n = 1$ bound state.

The sequence of forward surfing states $(\bar{2}, 0)$ displayed in figure 5(b) corresponds instead to *umklapp* processes involving the deepest level $n = 0$. More interesting is the long sequence $(\bar{1}, 0)_1$ of figure 5(a) observed at low incident angles and associated with *umklapp* surfing states in the $n = 1$ bound state level. Starting from $k_i = 5.33$ Å^{-1} down to 4.29 Å^{-1} the corresponding feature in the AD varies gradually with k_i from a dip to a peak and back to a dip. This behavior is well understood by looking at the plots (figure 6) of the corresponding resonant and scan curves with respect to the RW dispersion curve (also taken from [34]). The plot of figure 6(d) for $k_i = 4.91$ Å^{-1} and $\theta_i = 27.5°$ corresponds to a peak in the $(\bar{1}, 0)_1$ sequence and shows indeed the triple intersection of the $n = 1$ resonance curve with the scan and the RW dispersion curves yielding a *resonant focusing* (RF) [38, 46–48]. The triple intersection condition, leading to the RF maximum, is

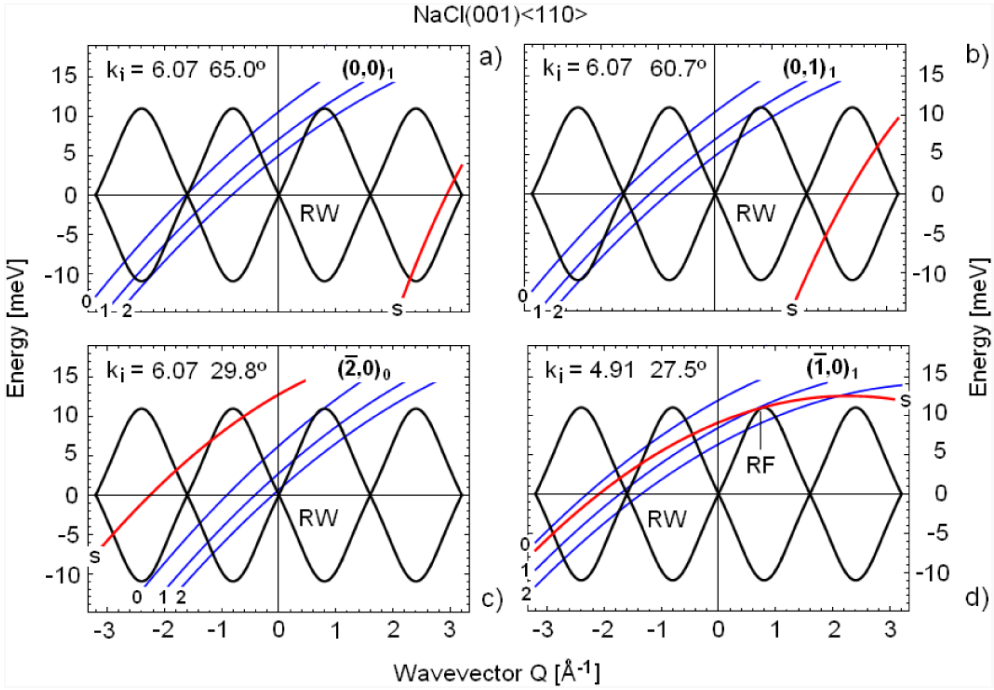

Figure 6. Same as figure 5 for NaCl(001) along the ⟨110⟩ direction for incident wavevectors (in Å^{-1}) and angles (degrees) corresponding to surfing states belonging to the four sequences shown in figure 5. A resonance curve which is tangent to the RW dispersion curve is labeled by the corresponding **G**-vector and bound state index as in figure 5. Note that the resonance curves for $n = 2$ in panels ((a), (b)) and $n = 0$ in panel (c) are tangent to the RW curve on the annihilation side (see section 3.3), which implies that the corresponding dips in the AD at the corresponding angles receive a contribution also from phonon annihilation processes. Panel (d) shows the intersection of the scan curve (s) with the tangency point on the $n = 1$ resonance curve; this yields a resonance focusing (RF) and a conversion of the surfing dip into a maximum along the focusing state sequence of figure 5(a).

approximately fulfilled within the natural resonance width and the incident momentum resolution over a fairly extended range of incident angles.

The other examples shown in panels ((a), (b), (c)) of figure 6 refer to the ordinary forward, oblique and *umklapp* surfing states for the highest value of k_i (see figures 5(c) and (d)), respectively, similar to those for NaF(001) displayed in figure 4. Note that the resonance curves for $n = 2$ in panels ((a), (b)) and $n = 0$ in panel (c) are tangent to the RW curve on the annihilation side. As discussed below (section 3.3), these tangency points also contribute to a dip in the AD. They, however, contribute a feature at the same incident energy and momentum as their companions on the creation side and therefore cannot be distinguished.

3.3. MgO(001)

Similar results are found from the analysis of the unexplained features in the existing ADs of LiF(001) [24] and MgO(001) [56] (see footnote 5). These crystals have a comparatively high RW frequency at the BZ boundary, comparable to the incident He beam energy used in the experiments. In these cases the surfing states are hardly seen on the creation side, but room temperature data provide evidence for the surfing effect on the annihilation side. These processes are necessarily *umklapp* because the energy of the atom in the bound state is larger than the incident energy. Classically the annihilation process cannot be visualized as real surfing because the RW has been destroyed by the arrival of the He atom, which continues its motion along the surface at the same speed. From the quantum point of view the sudden annihilation of one phonon leaves a transient track in the otherwise flat surface at thermal equilibrium, so that the surfing process can be viewed as a *phonon-hole riding*.

The HAS AD of MgO(001) shown in figure 7 has been measured at room temperature along the ⟨100⟩ direction with an incident energy (18.6 meV, $k_i = 6.00$ Å^{-1}) which is substantially smaller than the $\bar{M}$-point RW energy (33 meV) [56] (see footnote 5). At this incident energy the resolution is rather good and a wealth of resonant features are observed for incident angles between the specular and the diffraction peaks $(\bar{1}, \bar{1})$ and $(1, 1)$. There are also two small half-ordered diffraction peaks $\pm(1/2, 1/2)$ associated with a weak reconstruction. In the region of interest only seven inequivalent **G**-vectors contribute to SA. All possible SA resonances associated with some of the six known bound state levels ($\varepsilon_0 = -10.2$ meV, $\varepsilon_1 = -5.3$ meV, $\varepsilon_2 = -2.4$ meV $\varepsilon_3 = -0.90$ meV, $\varepsilon_4 = -0.55$ meV and $\varepsilon_5 = -0.20$ meV [56] (see footnote 5)) are marked in figure 7 and labeled with the surface **G**-vectors [56] (see footnote 5) and only a few sharp dips at 51.2°, 46.0° and 43.1°, and a doublet at 41° cannot be assigned to any SA.

The analysis in terms of surfing states (figure 8) indicates, as expected, that creation processes are only possible with the

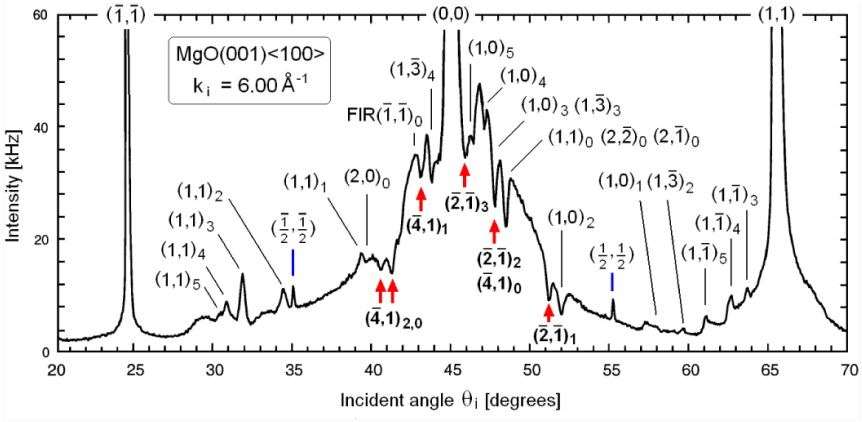

Figure 7. The AD of HAS from MgO(001) measured at room temperature along the ⟨100⟩ direction [56] (see footnote 5) showing the specular (0, 0) and diffraction ±(1, 1) peaks, the small satellite peaks ±(1/2, 1/2) associated with a weak surface reconstruction, and the rich structure of SA resonances (light-face labels) and surfing states (bold-face labels and thick upward arrows).

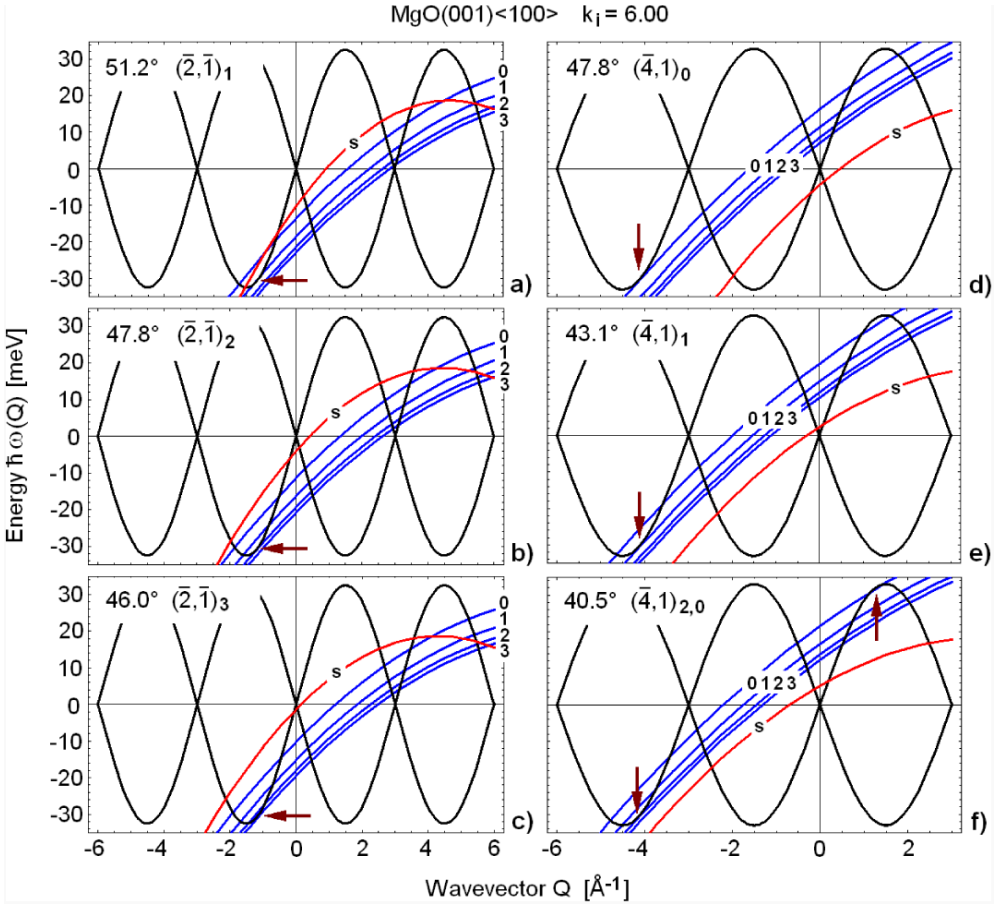

Figure 8. Same as figure 5 for MgO(001) for an incident wavevector of 6.00 Å^{-1} and the incident angles (degrees) marked by thick upward arrows in figure 7. These angles can be associated with two series of annihilation surfing states for $\mathbf{G} = (\bar{2}, \bar{1})_n$ (panels (a)–(c)) and $(\bar{4}, 1)$ (panels (d)–(f)). Tangency points are indicated by arrows. Panel (f) for $\theta_i = 40.5$ shows that two tangency points, one for creation and $n = 0$ and one for annihilation with $n = 2$, occur at almost the same angle, which may explain the doublet around 41° observed in the AD.

aid of fairly large **G**-vectors, whereas ordinary **G**-vectors only allow annihilation processes. It should be noted, however, that at room temperature, equivalent to 26 meV, the creation of an $\bar{M}$-point RW is only about twice as probable as annihilation, which fully justifies the search of annihilation surfing processes.

The plots of figure 8 suggest two series of possible surfing states, marked in figure 7 by bold-face labels and thick upward

arrows. The series $(\bar{2}, \bar{1})_n$ (figures 8(a)–(c)) permits us to assign the dips at 51.2° and 46.0° and to further contribute to the strong SA resonance at 47.8°. The $(\bar{2}, \bar{1})_0$ surfing state would instead fall about 57° where no significant dip is observed. The second series of possible surfing states, figures 8(d)–(f), provides an interpretation of the sharp dips at 43.1°, 40.6° and 41.5°, though with the rather exotic $\mathbf{G} = (\bar{4}, 1)$. Incidentally the doublet around 41° can be associated with a creation surfing state and an annihilation surfing state which occur at about the same angle with an $n = 0$ and 2 bound states, respectively (figure 8(f)). Clearly the present interpretation has no other purpose than illustrating the possible surfing processes which may occur. A firm assessment of the annihilation surfing states involving exotic **G**-vectors requires a high-resolution study of the ADs as functions of the incident wavevectors, as for NaCl(001), and/or slight azimuthal rotations as for NaF(001).

4. Discussion

The surfing effect has been analyzed in the previous sections on the basis of pure kinematics. There are, however, interesting physical issues raised by the existence of atom–phonon bound states traveling at the surface of crystals. The first question is: how long does the strange pair live? In the RF case the bound state is a scattering channel alternative to, and interfering with, the direct scattering process. Supposedly the peak width in the AD can be converted into a resonance lifetime, i.e. in a lifetime of the atom–phonon bound state. When the resonant conditions for RF are not met there is a question of decoherence related to the misfit of the two group velocities, mainly originating from the half-width of the velocity distribution of the incident atoms. Moreover anharmonicity and scattering from defects contribute to reduce the mean free path of the atom–phonon pair. The pure decoherence due to a relative spread $\Delta k_i/k_i \approx 0.5\%$ of the incident momentum would give a mean free path $\ell \approx \frac{1}{2}(k_i/\Delta k_i)\lambda_{RW}$. For an RW wavelength $\lambda_{RW} \approx 1$ nm, as found near the zone boundary where surfing states occur, it is $\ell \approx 100$ nm. This value is certainly less than one would expect from a good surfer, but interesting anyway for possible applications like phonon-assisted diffusion or selective dissociative adsorption of molecules [59]. This path length and the corresponding lifetime of ≈170 ps are, however, longer than, for example, the path lengths and lifetimes of the SA resonances for LiF(001) derived by Brusdeylins *et al* [60] from the measured SA peak half-widths. In that work (see table V of [60]), the residence times are found to be between 7 and 60 ps, corresponding to path lengths between 8 and 56 nm. Another interesting issue concerns the phonon energy renormalization due to the strong interaction with the atom, in practice a loading effect. The theory of the coupling of RWs to the dynamics of a mobile adsorbed atom has been developed long ago by means of the Hartree method [61]. This theory predicts a phonon energy renormalization which may be appreciable only at large Q, i.e. near the zone boundary, since the energy shift is found to vanish for $Q \to 0$ as Q^3. This is just a qualitative argument since the theory should actually be adapted to the case of an atom–phonon bound state.

Since the surfing states can be reached by an incident atom without exchanging a surface **G**-vector, and therefore the surface corrugation may not be needed, the surfing phenomenon, unlike elastic SA, could also be observed for particularly flat surface potentials like those of low-index metal surfaces. This would provide a tool for deriving the bound state levels also for metal surfaces. The ADs of low-index metal surfaces normally do not show any features besides the specular peak, though it should be noted that, to our knowledge, no specific investigation of possible weak features in the ADs has been carried out for metal surfaces. In direct ($\mathbf{G} = 0$) phonon-assisted SA and surfing processes the dynamic phonon-induced corrugation is surrogating the static corrugation needed for SA, and in the case of metals the dynamic corrugation is actually the phonon-induced surface charge density oscillations (SCDOs) [62]. As shown in [62] for Cu(111) the SCDOs at 3–4 Å away from the atom surface plane, where the He atom turning point is located at incident thermal energies, becomes appreciable for zone boundary surface phonons and give inelastic HAS intensities comparable to the HAS intensities for corrugated ionic surfaces. The amplitudes of the phonon-induced SCDOs are larger the larger is the electron–phonon interaction. Thus the surfaces of superconductors should offer the best conditions for the observation of He atoms surfing over the Fermi sea and high-resolution studies of HAS ADs in these systems may be worth the effort. On the theoretical side the calculation of the surfing amplitudes and lifetimes, as well as their effect on sticking and the Debye–Waller factor, could take advantage of recent progress in the theory of phonon-assisted resonances based on the RFCC approach [43–45] and on the knowledge of *ab initio* scattering potentials coupling He atoms to individual surface phonons [62].

The studies on the acoustoelectric effect quoted in the introduction, besides inspiring the present work, suggest a further extension to surfing phenomena in HREELS experiments. Resonance effects in electron surface scattering involving image bound states (surface Rydberg states [63]) have been known since the 1930s, exactly like bound state resonances in surface-atom scattering, and have received much attention in the last four decades following the development of HREELS [63–67]. The possibility of inelastic resonances involving either surface phonons or plasmons has been envisaged already in the classical review by McRae [64]. The subsequent experimental and theoretical works on resonance enhancement effects [68, 69], electron surface channeling [70], image-state resonance lifetimes [71], etc, of which just a few examples can be mentioned here, have largely contributed to the study of surface image states of conducting materials and adsorbates [67]. To our knowledge, however, no surfing effect has so far been detected in HREELS, despite the close similarity to inelastic SA phenomena observed in atom scattering. The self-trapping of charge carriers demonstrated by Ge *et al* experiments [16] can well be conceived for electrons injected from outside. Moreover other kinds of surface waves excited by incident electrons may be ridden, e.g. the surface acoustic plasmons on metal surfaces predicted by Silkin *et al* [72] and detected by HREELS by Diaconescu *et al*

[73], though the unusual pair, despite a favorable kinematics, may be allowed to live for only very short times, leaving a hardly detectable signature in the angular distributions.

Acknowledgments

One of the authors (GB) acknowledges the Ikerbasque Foundation for supporting the present research (project ABSIDES). A special thanks to Dick Manson for many illuminating suggestions during his stay at DIPC, watching the surfers' acrobatics in Zurriola Bay.

References

[1] Rocke C, Zimmermann S, Wixforth W, Kotthaus J P, Bohm G and Weiman G 1997 *Phys. Rev. Lett.* **78** 4009
[2] Willett R L, Ruel R R, West K W and Pfeiffer L N 1993 *Phys. Rev. Lett.* **71** 3846
[3] Talyanskii V I, Shilton J M, Pepper M, Smith C G, Ford C J B, Linfield E H, Ritchie D A and Jones G A C 1997 *Phys. Rev.* B **56** 15180
[4] Dunford R B, Gates M R, Mellor C J, Rampton V W, Chauhan J S, Middelton J R and Henini M 2002 *Physica* E **12** 462
[5] Totland T, Bø Ø L and Galperin Y M 1997 *Phys. Rev.* B **56** 15299
[6] Alsina F, Santos P V, Schönherr H-P, Nötzel R and Ploog K H 2004 *Physica* E **21** 430
[7] Kleinert P, Garcìa-Cristòbal A and Santos P V 2005 *Solid State Commun.* **134** 535
[8] Cecchini M *et al* 2004 *Appl. Phys. Lett.* **85** 3020
Cecchini M *et al* 2005 *Appl. Phys. Lett.* **86** 241107
Cecchini M *et al* 2006 *Appl. Phys. Lett.* **88** 212101
[9] Gell J R, Ward M B, Atkinson P, Bremmer S P, Anderson D, Norman C E, Kataoka M, Barnes C H W, Jones G A C, Shields A J and Ritchie D A 2008 *Physica* E **40** 1775
[10] Rodriquez R, Oi D K L, Kataoka M, Barnes C H W, Oshima T and Ekert A K 2005 *Phys. Rev.* B **72** 085329
[11] Kataoka M, Schneble R J, Thorn A L, Barnes C H W, Ford C J B, Anderson D, Jones G A C, Farrer I, Ritchie D A and Pepper M 2007 *Phys. Rev. Lett.* **98** 046801
[12] Bertoni A, Bordone P, Brunetti R, Jacoboni C and Reggiani S 2000 *Phys. Rev. Lett.* **84** 5912
[13] Barnes C H W 2003 *Phil. Trans. R. Soc.* A **361** 1487
[14] Furuta S, Barnes C H W and Doran C J L 2004 *Phys. Rev.* B **70** 205320
[15] Piazza V, De Simoni G, Strambini E, Cecchini M and Beltram F 2005–2006 *SAW-Driven Opto-Electronic Devices* (Pisa: NEST Sci. Rep.) p 41
[16] Ge H N, Wong C M, Lingle R L Jr, McNeill J D, Gaffney K J and Harris C B 1998 *Science* **279** 202
[17] Benedek G and Toennies J P 1994 *Surface Science: The First Thirty Years* ed C B Duke (Amsterdam: Elsevier)
Benedek G and Toennies J P 2010 *Helium Atom Scattering Spectroscopy of Surface Phonons* (Berlin: Springer) in preparation
[18] Ibach H and Mills D L 1982 *Electron Energy Loss Spectroscopy and Surface Vibrations* (New York: Academic)
[19] Ibach H 2007 *Physics of Surfaces and Interfaces* (Berlin: Springer) chapter 7
[20] Manson J R and Celli V 1971 *Surf. Sci.* **24** 485
[21] Manson J R 1991 *Phys. Rev.* B **43** 6924
[22] Celli V 1992 *Surface Phonons* ed F W de Wette and W Kress (Berlin: Springer) chapter 6
[23] Brusdeylins G, Doak R B and Toennies J P 1980 *Phys. Rev. Lett.* **44** 1417
Brusdeylins G, Doak R B and Toennies J P 1981 *Phys. Rev. Lett.* **46** 437
[24] Brusdeylins G, Doak R B and Toennies J P 1983 *Phys. Rev.* B **27** 3662
[25] Toennies J P 1991 *Surface Phonons* (*Springer Series in Surface Sciences* vol 21) ed F W deWette and W Kress (Berlin: Springer) pp 111–66
[26] Gumhalter B 2001 *Phys. Rep.* **351** 1
[27] Benedek G 1975 *Phys. Rev. Lett.* **35** 234
[28] Cantini P, Felcher G P and Tatarek R 1976 *Phys. Rev. Lett.* **37** 606
[29] Lilienkamp G and Toennies J P 1982 *Phys. Rev.* B **26** 4752
[30] Evans D, Celli V, Benedek G, Toennies J P and Doak R B 1983 *Phys. Rev. Lett.* **50** 1854
[31] Benedek G, Toennies J P and Doak R B 1983 *Phys. Rev.* B **28** 7277
[32] Benedek G, Brusdeylins G, Toennies J P and Doak R B 1983 *Phys. Rev.* B **27** 2488
[33] Benedek G and Miret-Artés S 1995 *Surf. Sci.* **339** L935
[34] Benedek G, Gerlach R, Glebov A, Lange G, Miret-Artés S, Skofronick J G and Toennies J P 1996 *Phys. Rev.* B **53** 11211
[35] Bertino M F, Miret-Artés S, Toennies J P and Benedek G 1997 *Phys. Rev.* B **56** 9964
[36] Glebov A, Manson J R, Miret-Artés S, Skofronick J G and Toennies J P 1998 *Phys. Rev.* B **57** R9455
[37] Šiber A, Gumhalter B, Graham A P and Toennies J P 2001 *Phys. Rev.* B **63** 115411
[38] Miret-Artés S 1996 *Surf. Sci.* **366** L735
[39] Šiber A and Gumhalter B 1998 *Phys. Rev. Lett.* **81** 1742
[40] Šiber A, Gumhalter B and Wöll C 2002 *J. Phys.: Condens. Matter* **14** 5913
[41] Brenig W 2004 *Phys. Rev. Lett.* **92** 056102
[42] Brenig W and Gumhalter B 2004 *J. Phys. Chem.* B **108** 14549
[43] Šiber A and Gumhalter B 2005 *Phys. Rev.* B **71** 081401
[44] Šiber A and Gumhalter B 2007 *Phys. Rev.* B **75** 046402
[45] Šiber A and Gumhalter B 2008 *J. Phys.: Condens. Matter* **20** 224002
[46] Hernández M, Miret-Artés S, Villarreal P and Delgado-Barrio G 1992 *Surf. Sci.* **274** 21
[47] Miret-Artés S 1993 *Surf. Sci.* **294** 141
[48] Miret-Artés S 1995 *Surf. Sci.* **339** 205
[49] Miret-Artés S 1999 *Phys. Rev.* B **60** 1547
[50] Miret-Artés S and Manson J R 1999 *Phys. Rev.* B **60** 6080
[51] Miret-Artés S and Manson J R 2001 *Phys. Rev.* B **63** 121404
[52] Brusdeylins G, Rechsteiner R, Skofronick J G, Toennies J P, Benedek G and Miglio L 1985 *Phys. Rev. Lett.* **54** 466
[53] Bracco G, Tatarek R, Terreni S and Tommasini F 1986 *Phys. Rev.* B **34** 9045
[54] Brusdeylins G, Doak R B and Toennies J P 1981 *J. Chem. Phys.* **75** 1784
[55] Benedek G, Brusdeylins G, Doak R B, Skofronick J G and Toennies J P 1983 *Phys. Rev.* B **28** 2104
[56] Benedek G, Brusdeylins G, Senz V, Skofronick J G, Toennies J P, Traeger F and Vollmer R 2001 *Phys. Rev.* B **64** 125421
[57] Alexandrov A S and Devreese J T 2010 *Advances in Polaron Physics* (Berlin: Springer)
[58] Benedek G, Glebov A, Silvestri W, Skofronick J G and Toennies J P 1997 *Surf. Sci. Lett.* **381** L540
Benedek G, Glebov A, Silvestri W, Skofronick J G and Toennies J P 1998 *Surf. Sci. Lett.* **406** L621
[59] Nieto P, Pijper E, Barredo D, Laurent G, Olsen R A, Baerends E G, Kroes G J and Farias D 2006 *Science* **312** 86
[60] Brusdeylins G, Doak R B and Toennies J P 1983 *J. Chem. Phys.* **75** 1784
[61] Benedek G and Brivio G P 1976 *J. Phys. C: Solid State Phys.* **9** 2709
[62] Chis V, Hellsing B, Benedek B, Bernasconi M, Chulkov E V and Toennies J P 2008 *Phys. Rev. Lett.* **101** 206102

Chis V, Hellsing B, Benedek B, Bernasconi M, Chulkov E V and Toennies J P 2009 *Phys. Rev. Lett.* **103** 069902
[63] Echenique P M and Pendry J B 1978 *J. Phys.* C **11** 2065
[64] MaRae M G 1979 *Rev. Mod. Phys.* **51** 541
[65] Willis R F 1982 *Vibrations at Surfaces* ed R Caudano, J-M Gilles and A A Lucas (New York: Plenum) p 153
[66] Palmer R E and Rous P J 1992 *Rev. Mod. Phys.* **64** 383
[67] Šiller L and Palmer R E 1999 *Supercomputing, Collision Processes, and Applications* ed K L Bell, K A Berrington, D S F Crothers, A Hibbert and K T Taylor (New York: Kluwer Academic/Plenum) p 197
[68] Conrad H, Kordesch M E, Scala R and Stenzel W 1986 *J. Electron Spectrosc. Relat. Mater.* **38** 289
[69] Conrad H, Kordesch M E, Stenzel W, Sunjič M and Trninic-Radia B 1986 *Surf. Sci.* **178** 578
[70] Peng L-M and Cowley J M 1988 *Surf. Sci.* **204** 555
[71] Borisov A G, Chulkov E V and Echenique P M 2006 *Phys. Rev.* B **73** 073402
[72] Silkin V M, Pitarke J M, Chulkov E V and Echenique P M 2005 *Phys. Rev.* B **72** 115435
[73] Diaconescu B, Pohl K, Vattuone L, Savio L, Hofmann Ph, Silkin V M, Pitarke J M, Chulkov E V, Echenique P M, Farias D and Rocca M 2007 *Nature* **448** 57